applied sciences

MDPI

Article

Evaluation of Water Vapor Diffusion of Empress Tree Hybrid Samples with Adhesive

Omar Saber Zinad * and Csilla Csiha

Faculty of Wood Engineering and Creative Industries, University of Sopron, 9400 Sopron, Hungary; csiha.csilla@uni-sopron.hu

* Correspondence: omar.saber.khalaf.zinad@phd.uni-sopron.hu

Abstract

In Hungary, a fast-growing Empress tree hybrid (×*Paulownia Clone* in vitro *112*) also known as Smaragdfa® has been developed as a low-density plantation species seeking industrial utilization. Many potential industrial applications presuppose its bonding. The presence of adhesives in bonded layered assemblies, with differing climatic conditions on the internal and outer side, may induce undesired internal strains due to restricted water vapor diffusion, especially in the case of Smaragdfa as a low-density wood species. For decades, lasures have been specifically formulated with a molecular structure that allows partial vapor transmission while hindering water diffusion. Lasure-coated samples were used as control samples to identify, among the different custom-made MW adhesives, the one with diffusion properties closest to those of the lasure. Uncoated Smaragdfa wood samples were used as the baseline reference to evaluate the effect of different adhesive and coating systems on water vapor diffusion. Smaragdfa samples were prepared both uncoated and coated with different adhesive and lasure layers. Experiments were conducted following ISO 12572 and ASTM E96 standards using the cup method, with all specimens pre-conditioned to 12% moisture content. Results showed that the uncoated Smaragdfa exhibited the highest diffusion coefficient ($\delta = 7.02 \times 10^{-13}$ kg/(m·s·Pa)) and flow rate (G = 0.055763 g/h), while the commercial adhesive-coated sample displayed an 84% reduction in diffusion capacity ($\delta = 1.15 \times 10^{-13}$ kg/(m·s·Pa)), indicating a strong vapor-blocking effect. The lasure coating allowed partial vapor transmission, confirming its semi-permeable nature. Adhesives formulated with varying polyol molecular weights (Series 1–5) revealed a clear molecular-weight-dependent diffusion behavior: low-MW systems (S1) acted as strong diffusion barriers comparable to lasure-coated samples (SMW_L), in the same time high-MW systems (S4, S5) permitted excessive diffusion but induced microcracking, while intermediate formulations (S2, S3) achieved the most balanced performance, combining moderate diffusion with structural stability. Overall, the findings confirm that adhesive layers significantly influence water vapor transmission through Smaragdfa wood, with the degree of hindrance closely related to the molecular weight of the polyol matrix. The optimized formulations (S2, S3) demonstrate promising potential for use in bonded assemblies and engineered wood products where controlled vapor diffusion and mechanical reliability are critical in order to support reduced strains caused by water vapor.

Keywords: water vapor diffusion; adhesive; steady state zone; pre-steady zone

Academic Editors: Lidia Gurau, Mihaela Câmpean and Emilia-Adela Salca

Received: 13 February 2026
Revised: 17 March 2026
Accepted: 18 March 2026
Published: 20 March 2026

1. Introduction

The global transition toward sustainable construction materials has intensified scientific interest in renewable, carbon-storing alternatives that can reduce environmental

emissions associated with the production of common construction materials, such as cement, concrete, and steel. Engineered wood products (EWPs) offer a promising solution, offering advantages in resource efficiency, structural performance, and reduced greenhouse gas emissions [1,2].

Generally, wood is a hygroscopic material and is continuously affected by surrounding moisture, leading to swelling, shrinking, and internal stresses caused by dimensional instability and construction performance for EWPs [3–5]. Despite the research efforts remaining largely concentrated on a limited number of commercially established species familiar to researchers, such as spruce, Scots pine, and beech, there remain numerous wood species that have not yet been sufficiently investigated to determine their suitability for engineering applications. Consequently, studying the engineering properties of the Empress tree hybrid (×*Paulownia Clone* in vitro *112*) has become increasingly important; in particular, evaluating its behavior with respect to moisture-related diffusion properties that can affect the overall performance of bonded in layer wood products form this wood species.

The Empress tree hybrid (×*Paulownia Clone* in vitro *112*), as a fast-growing plantation wood species, also known as Smaragdfa® (SMW), has been producing hybrid paulownia seedlings by micropropagation since 2003. It is a clone selected and tested in the field, by In Vitro SL, for more than 10 years, it is not a genetically modified organism (GMO), since it comes from a natural cross. It produces perfectly cylindrical and straight trunks and concentric rings [6,7].

With most particularly PUR, phenolic systems, and EPI formulations, it was already demonstrated that they are resistant to water vapor transmission due to their dense polymer networks and high molecular weight. As a result, moisture accumulates asymmetrically, for example, in CLT exposed to external humidity gradients. These blocked diffusion pathways create stress concentrations at the adhesive interface, increasing risks of delamination, microcracking, and long-term deterioration of CLT assemblies [8]. The adhesive layer might affect water vapor diffusion, in cases where the diffusion parameters of the adhesive are different than those of the wood. The more significant the difference in favor of adhesive, the more the layer acts as a barrier, even blocking the diffusion of water vapor. Even in cases where the water vapor diffusion is not completely blocked, but hindered, internal stresses begin to develop within the wood. These stresses arise due to the partial penetration of fine water vapor particles through the adhesive toward the wood, inducing its swelling, while a substantial portion of the vapor is obstructed. This unequilibrated diffusion results in differentiated stress at the interface between the adhesive layer and the wood substrate [8].

This study investigates water vapor diffusion through SMW, SMW_{AJ}, SMW_{AX}, SMW_{L}, and SMW with a series of custom-made synthesized adhesive resins ($SMWS_i$, i = 1–5). Sample preparation and experiments were conducted under controlled hot-steam environmental conditions using the cup method, and the results were evaluated according to the first Fick's law for steady-state conditions [9–11]. Although water diffusion in various wood species has been extensively described over the past six decades, water vapor diffusion through SMW, as well as through different custom-made synthesized adhesive layers applied to SMW, has not yet been reported in the literature. The availability of such quantitative diffusion data and related insights into water vapor diffusion through adhesive layers may enhance the broader knowledge base on this unique wood species and support its industrial utilization. This aspect becomes particularly relevant in applications such as door and window production, CLT production, etc., where differences in vapor diffusion behavior across bonded layers may lead to moisture gradients, internal stress development, and potential structural failure. Consequently, the identification or development of adhesive systems that allow controlled water vapor diffusion may play a key role in adhesive design, production and manufacturing.

2. Materials and Methods

2.1. Material

Smaragdfa® (SMW) (×*Paulownia Clone* in vitro *112*), as shown in Figure 1, is a fast-growing, plantation-grown hybrid that is a lightweight raw material with an average dry density of approximately 380 kg/m^3, measured in this study. SMW is characterized by high porosity, large vessels, and thin-walled fibers, which distinguish it from conventional hardwoods and softwoods. These anatomical features result in low hardness and pronounced swelling and shrinkage even under minor changes in water vapor. Its high sensitivity to moisture makes it a perfect candidate for the investigation of moisture induced dimensional changes, supporting reliable detection of moisture diffusion effects, which justifies its classification as a low-strength wood species [12]. All boards were taken from a uniform region and conditioned to a moisture content of 10.8–12% at 20–21 °C and 65% RH prior to testing. Disk-shaped specimens with a thickness of 10 mm were prepared using a 10 cm diameter crown saw, with the thickness direction oriented parallel to the grain to ensure consistent vapor transport conditions.

Figure 1. Smaragdfa® wood (×*Paulownia Clone* in vitro *112*).

Structural Adhesives JOWAPUR 681-60 (AJ) (Jowat SE Co., Detmold, Germany). This adhesive is a joint-filling, fiber-reinforced, one-component commercial polyurethane adhesive specifically designed for load-bearing wood structures and it is commercially available. According to the data sheet provided by Jowat SE, the amount used in this study was 150 g/m^2 at a temperature of 20 °C, a wood MC 12%, and an RH 65%.

Adhesive XP 1166 (Ax): was a custom-made adhesive available at BorsodChem Ltd. (BorsodChem Zrt., Kazincbarcika, Hungary), under the name Original XP 1166, with brown color and high viscosity, it was used with an application amount of 150 g/m^2.

Ajtó és ablaklazúr OBI: lasures are penetrative but film-forming wood finishes proposed for outdoor use in Europe, and also in Hungary, due to their specially designed molecule size and structure which offer control over promoted water vapor permeability parallel with hindering the water uptake through the layer, enabling a promoted vapor permeability associated with a moderate water uptake. Several studies have demonstrated the effectiveness of lasures in reducing moisture uptake and improving UV resistance [13]. The lasure used for experiments was purchased from OBI Hungary (Sopron, Hungary), with a density of 1300 g/L, and contains binders (linseed oil and acrylic polymers), pigments (iron oxides and titanium dioxide), solvent, and aqueous phases for application. It

allows water vapor diffusion but has high resistance to water absorption. It was applied by a spongy roller with an application amount of 150 g/m^2.

Custom-made synthesized resin series (Si; i = 1–5): five custom-made adhesives specially designed to these experiments were formulated with different MWs by BorsodChem Gödöllő (Hungary). These resins were synthesized through controlled variation in the MW and structure of polyether polyols (PPG diols and triols), specifically by modifying the MW. All samples contained free monomeric MDI (methylene diphenyl isocyanate) and structurally distinct prepolymer. The MDI component used in these formulations consisted solely of monomeric MDI, devoid of high-molecular-weight oligomers. Table 1 and Figure 2.

Table 1. Custom-made synthesized polymers used according to the manufacturer.

Series	Mixing Ratio (%)	Average MW
Series 1 (S1)	100% (2000 Mw Diol)/0% (6000 Mw Triol)	2000
Series 2 (S2)	75% (2000 Mw Diol)/25% (6000 Mw Triol)	3000
Series 3 (S3)	50% (2000 Mw Diol)/50% (6000 Mw Triol)	4000
Series 4 (S4)	25% (2000 Mw Diol)/75% (6000 Mw Triol)	5000
Series 5 (S5)	0% (2000 Mw Diol)/100% (6000 Mw Triol)	6000

Figure 2. (**Left**) side: samples prepared according to ISO 12572 and the 5 custom made polyol formulations with different molecular weights and the custom made adhesive; (**right**) side: cups with the Smaragdfa disks coated with the listed polymers.

By adjusting the molecular weight (MW) of the synthetic resin formulations, the polyol systems were conceptually modified, resulting in different water vapor diffusion while hindering liquid water uptake through the adhesive layer. This design approach was inspired by the manufacturing concept of lasures, which are known to allow controlled vapor permeability while restricting liquid water penetration. The underlying hypothesis assumes that the diffusion behavior can be tailored through precise control of the adhesive's molecular size, enabling selective permeability toward water vapor while limiting liquid water transport.

The polyurethane-based adhesive systems used in this study are commonly designed for structural and exterior wood applications and exhibit resistance to short-term water exposure.

Silica gel: FIO-1533 type indicator-type silica gel (Fiorex Packaging Kft., Budapest, Hungary) was used in granular form. Its color change from orange to green upon moisture saturation served as a qualitative indicator of environmental humidity.

Sealing materials: LOCTITE® SI 5699 gray silicone sealant (Henkel) was used to create a vapor-tight seal between the aluminum cup and the wood specimen, ensuring the integrity of the vapor diffusion measurements.

2.2. Experimental Work

2.2.1. Sample Preparation

The SMW samples were obtained from healthy, defect-free trees without knots or decay. Boards were cut from a radial position to ensure uniform grain orientation. The specimens were conditioned at 40 °C to reach an equilibrium moisture content of approximately 12%, then sanded to a uniform thickness of 10 mm by using a sanding machine, Aligator 630 by HOUFEK Co., Czech Republic, with sanding paper of grit size P150, to obtain a uniform surface prior to coating application, since surface preparation influences the penetration of the resins into the wood structure [14]. After dedusting, one surface of the specimens was coated with either lasure, commercial structural adhesives, or custom-made synthesized adhesive with a sponge roller to achieve a uniform, bubble-free layer, with a target application rate of 150 g/m^2. Adhesives were applied in three thin, consecutive layers with 120 s intervals, and the adhesive was allowed to cure for 24 h. The thickness of the final adhesive-coating layer was not directly measured; instead, the application rate was regulated according to the manufacturer's recommendations to ensure comparable coating conditions among the specimens.

Disk-shaped specimens (100 mm diameter, 10 mm thickness) were prepared, acclimatized to 12 ± 0.5% moisture content, and tested using the cup method according to ISO 12572:2016 [15] and ASTM E96/E96M [16]. Aluminum cups were filled with silica gel and sealed to the specimen edges using silicone. The tests were conducted in an airtight, heated vapor chamber; this chamber was an out-of-function 240 L refrigerator, conveniently modified for experimental purposes. Inside the chamber, a water boiler continuously generated hot steam at 100 °C. The cups were placed top-down on a metallic grid at a distance of 75 cm from the steam source. The metal grid holding the cups was tilted by 15° to support the continuous skidding of condensed water precipitation from the sample surfaces. The temperature and the RH inside the chamber were continuously monitored. Throughout the test, RH reached 100%, and the temperature remained close to 70 °C at the sample level.

Mass changes were recorded periodically over this accelerated diffusion period, and diffusion coefficients were calculated for comparative evaluation of the coating systems. Each specimen was numbered and weighed periodically, and 90 samples were introduced into the steaming chamber at a time. Over 20 systematic measurements were taken for each sample across a total test duration of approximately 22,500 min (15.6 days), with the measurements for individual samples shifted with the same time interval. During each measurement, a sample was quickly removed from the chamber, surface moisture was gently wiped off using a highly absorbent paper towel, and the specimen was weighed within 20 s. To minimize environmental disruption, the chamber door was opened for less than 5 s each time, with at least a 20 min interval between openings to allow internal conditions to stabilize before the next measurement.

2.2.2. Measuring the Water Vapor Permeability Through the Adhesive Layer

Moisture diffusion is traditionally evaluated using Fick's first and second laws of diffusion [17], which can be expressed as,

First Law steady state:

$$J = -D_{\propto}\frac{\partial \propto}{\partial x} \quad (1)$$

Second Law transient

$$\frac{\partial \propto}{\partial t} = \frac{\partial}{\partial x}\left(D_{\propto}\frac{\partial \propto}{\partial x}\right) \quad (2)$$

where $D_\propto$ is the diffusion coefficient with the parameter $\propto$ referring to the driving potential for moisture diffusion, which in this study is the water vapor concentration (or partial vapor pressure) gradient [18].

There are two widely spread standards used for the evaluation of water vapor diffusion of anisotropic materials: ISO 12572:2016 and ASTM E95/96M. Both standards characterize the diffusion by the diffusion coefficient, with similar principles:

The water vapor permeability, calculated by Equation (3).

$$\delta = \mathrm{Wd}\ (\mathrm{kg}/(\mathrm{m}\cdot\mathrm{s}\cdot\mathrm{Pa})) \tag{3}$$

Water vapor permeability (δ) is the mass of water vapor that diffuses through a material of unit thickness, per unit area, per unit time, per unit vapor pressure difference. The parameter d represents the specimen thickness.

Where t is the time (in s), G is the mass change rate (in kg), A is the surface area of the specimen (in m^2), Ps is the saturation vapor pressure (in Pa), RH is the relative humidity (unitless), and d is the average thickness of the specimen (in m).

The water vapor permeance W can be calculated by

$$W = \frac{g}{\Delta p}\ (\mathrm{kg}/(\mathrm{m}^2\cdot\mathrm{s}\cdot\mathrm{Pa})) \tag{4}$$

The change in vapor pressure (Δp) can be estimated as a function of temperature (T, °C) by Tetens Equation [19]

$$p = 610.5e^{\left(\frac{17.27T}{T+237.3}\right)} \tag{5}$$

$$\Delta p = (Ps * RH2) - (Pa * RH1) \tag{6}$$

The water vapor flow rate: g, can be calculated by

$$g = \frac{G}{A}\ (\mathrm{kg}/\mathrm{s}\cdot\mathrm{m}^2) \tag{7}$$

where A is the exposed area (arithmetic mean of the inside and outside surface areas of the disklike samples free of silicone, in m^2). The mass change rate per time was calculated based on the following equation:

$$G = \frac{m_2 - m_1}{t_2 - t_1}\ (\mathrm{kg}/\mathrm{s}) \tag{8}$$

Further to the calculation of the mass change rate, this modeling approach leads to the determination of the transition point "A" between the non-linear (pre-steady) and linear (steady) regions of the diffusion curve.

The segment preceding this transition point was defined being the pre-steady zone, while the linear portion that followed point G was identified being the steady zone as in ASTM E95/96 and ISO 12572/2016. The difference between these two standards is that in ASTM E95/96 the mass change rate is defined as the slope of the steady zone of the diffusion curve, whilst in ISO 12572/2016 the final value of G is obtained when the mean of the last five successive determinations is within ±5% of G, indicating that the diffusion reached the steady state. For our measurements, G was identified using the ASTM method (Equation (8)), and the ISO expectations were also met.

The diffusion test included five specimens per type, and the average change in mass was calculated for each type. For Equation (6), the RH1 in our case was zero, as the relative humidity above the silica gel inside the cup was zero. For our experiments, RH2 was 100%, the relative humidity inside the chamber.

The weight measurements for all specimens were recorded at short intervals to ensure consistent measurement conditions.

The coatings and adhesive systems used in this study are based on polyurethane and MDI-containing formulations typically designed for structural wood applications and are stable at temperatures above the experimental range used in this work. Therefore, the applied temperature (~70 °C) was not expected to exceed the glass transition temperature of the cured adhesive systems or significantly alter their diffusion behavior.

To support the analysis of mass change behavior over time, Statistica V2025 software was employed to identify the trend line that best represented the relationship between mass change and exposure time, automatically selecting the most appropriate function based on goodness-of-fit criteria. This software also enabled the determination of the transition point "A" between the non-linear (pre-steady) and linear (steady) regions of the diffusion curve.

3. Results and Discussion

The diffusion process consisted of an initial pre-steady stage, symbolized by point "A (x_A; y_A)" on Figures 3 and 4 transitioning into a steady zone for SMW, which provided the basis for deriving curve slopes and quantifying both diffusion coefficients and vapor flow rates.

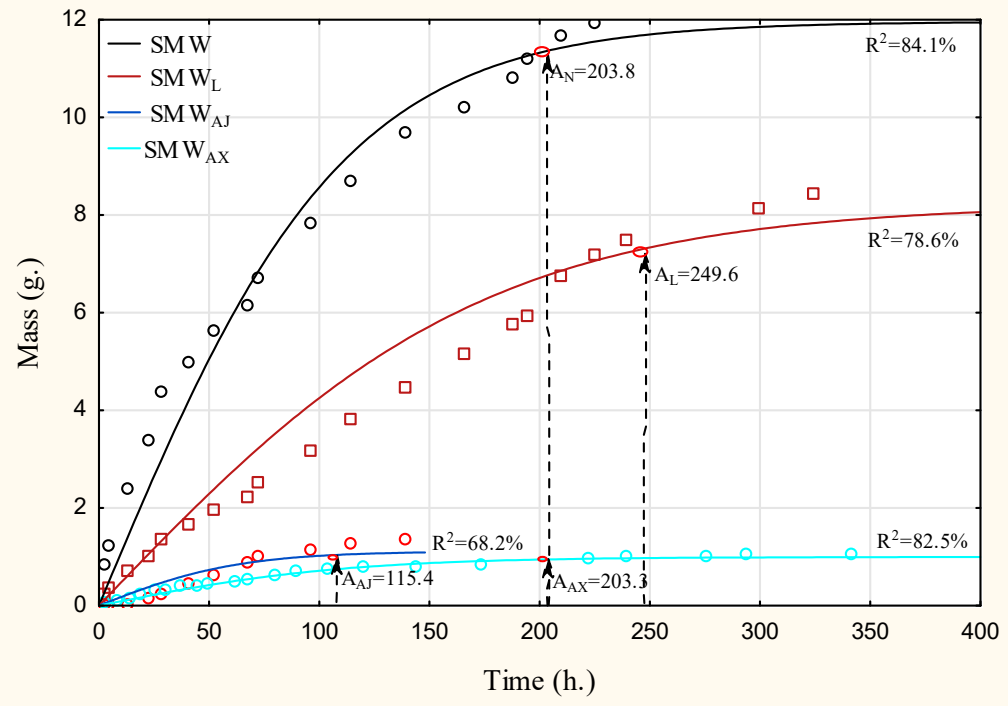

Figure 3. The mass change over time for SMW, SMW$_L$, SMW$_{AJ}$ and SMW$_{AX}$.

The lowercase letter (s) denotes results obtained in the steady-state zone, whereas (p) denotes results obtained in the pre-steady zone; thus, identical sample designations (e.g., SMW, SMW$_{AJ}$, SMW$_{AX}$, SMW$_L$, SMW$_{S1}$–SMW$_{S5}$) are labeled with s or p solely to distinguish the evaluation stage of diffusion.

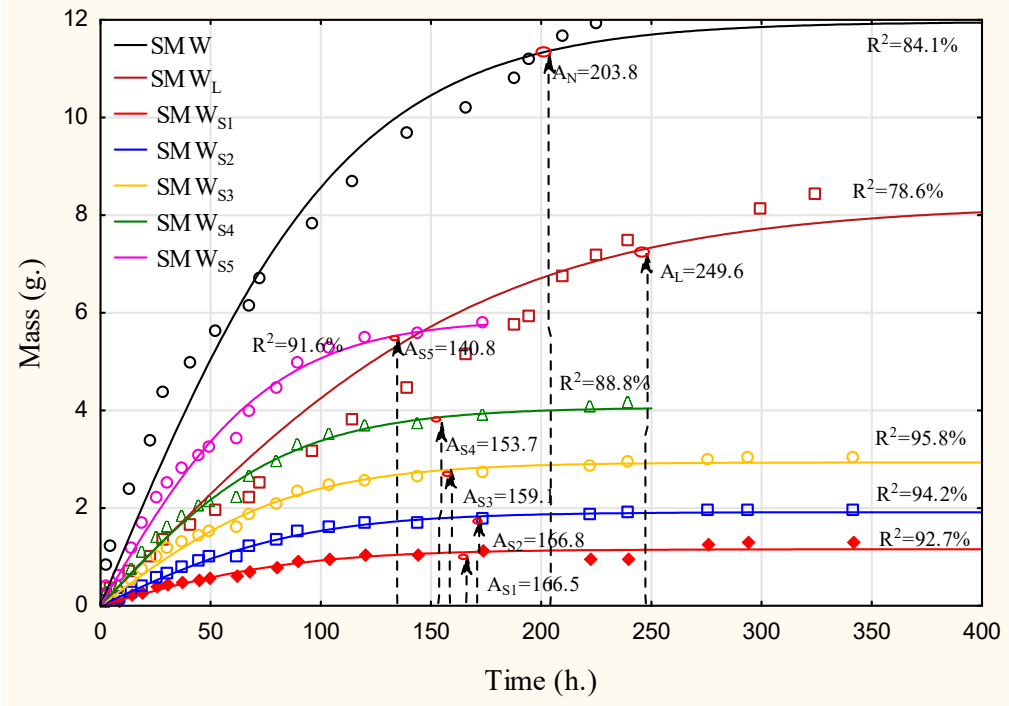

Figure 4. The mass change over time for SMW$_L$, SMW$_{S1}$, SMW$_{S2}$, SMW$_{S3}$, SMW$_{S4}$, and SMW$_{S5}$.

3.1. Water Vapor Diffusion for SMW in the Steady Zone

According to ASTM E96 and ISO 12572 the diffusion coefficient parameters are calculated depending on the slope of the curve line that is shown in Figures 3 and 4.

According to Table 2, in the steady zone, SMW shows a water vapor permeability of $\delta = 3.721956 \times 10^{-14}$ kg/(m·s·Pa) and a water vapor flow rate of G = 0.002954 g/h, whereas SMAJ$_S$ exhibits a much lower water vapor permeability of $\delta = 0.248 \times 10^{-14}$ kg/(m·s·Pa) and a flow rate of G = 0.000197 g/h. For both SMWs and SMW$_{AJs}$, a clear, approximately 15-fold difference can be observed in δ and G; a one-way ANOVA revealed a statistically significant difference in the water vapor permeability coefficient δ between SMW and SMW$_{AJS}$ ($F(1, 8) \approx 520$, $p < 0.041$), confirming the pronounced vapor-blocking effect of the commercial adhesive layer.

The mass change in SMW at transition point A in the steady zone was = 1.05 g within 115.4 h, but for the SMW$_{AJS}$, the mass change was recorded = 11.4 g within 203.8 h at the same point. This comparison reveals a substantial difference in the vapor diffusion behavior of the natural Smaragdfa® and the adhesive-coated samples. This leads to the conclusion that the commercial adhesive has a strong hindrance to water vapor diffusion. This behavior is consistent with previous studies reporting that adhesive layers can significantly reduce vapor permeability by modifying the moisture transport pathways within bonded wood systems [20,21].

As shown in Table 2, the diffusion parameters G and δ for SMW$_{LS}$ were approximately 1.64 times higher than those of SMW and about 24.5 times higher than those of SMW$_{AJS}$. The transition point for SMW$_{LS}$ was reached after 249.6 h of testing with a mass change of 7.33 g, compared to SMW, which reached its transition point after 203.8 h with a mass change of 11.364 g, and SMW$_{AJS}$, which reached the transition point after 115.4 h with only 1.053 g. This indicates a broadly similar steady-state time for the diffusion process relative to the SMW, albeit with a substantially lower total mass gain. The higher vapor diffusion observed in SMWL$_S$ compared to SMW$_{AJS}$ suggests that the lasure layer permits partial vapor diffusion, likely facilitated by its capillary structure induced by its molecular weight. Similar behavior has been reported for surface coatings with semi-permeable

molecular structures where the coating limits but does not completely block vapor diffusion through the substrates [22]. Similarly, the molecular weight of the custom-made synthesized polymers can also be formulated to keep the permeability under control, as shown below.

Table 2. Water vapor diffusion parameters of Smaragdfa wood samples in steady and pre-steady zone.

Sample	x_A (h)	y_A (g)	G (g/h)	$W \times 10^{-12}$ kg/(m^2·s·Pa)	$\delta \times 10^{-14}$ kg/(m·s·Pa)
SMW_S	203.8	11.3644	0.002954	3.721956	3.721956
SMW_P			0.055763	70.24797	70.24797
SMW_{AJS}	115.4	1.0531	0.000197	0.248756	0.248756
SMW_{AJP}			0.009126	11.49712	11.49712
SMW_{AXS}	203.3	0.9458	0.000246	0.309423	0.309423
SMW_{AXP}			0.004653	5.861104	5.861104
SMW_{LS}	249.6	7.3323	0.004840	6.096917	6.096917
SMW_{LP}			0.029376	37.00682	37.00682
SMW_{S5S}	140.8	5.5862	0.001133	1.427151	1.427151
SMW_{S5P}			0.039675	49.981	49.981
SMW_{S4S}	153.7	3.8595	0.000822	1.035292	1.035292
SMW_{S4P}			0.025111	31.63383	31.63383
SMW_{S3S}	159.1	2.7886	0.000607	0.765289	0.765289
SMW_{S3P}			0.017527	22.08042	22.08042
SMW_{S2S}	166.8	1.8211	0.000409	0.514957	0.514957
SMW_{S2P}			0.010918	13.75439	13.75439
SMW_{S1S}	166.5	1.0983	0.000246	0.310181	0.310181
SMW_{S1P}			0.006597	8.310287	8.310287

Low-MW polyols, like S1 and S2 together with AX, produced the most pronounced resistance to water vapor diffusion. The permeability of these systems was reduced by approximately 80–85% compared with SMW, remaining very close to SMW_{AJ}. Correspondingly, the vapor flow rate was also substantially reduced, and stabilization occurred relatively early (153.9–198.7 h), indicating the formation of an almost continuous vapor barrier comparable to that produced by the commercial adhesive layer. A one-way ANOVA revealed a statistically significant difference in the water vapor permeability coefficient δ among the SMW surface treatments ($F(3, 16) \approx 41.8$, $p < 0.011$), confirming the pronounced vapor-blocking behavior of the low-molecular-weight formulations and AX compared with SMW.

Intermediate-MW polyol formulation S3 allowed moderate permeability with a transition point at 159.1 h and a mass uptake of 5.19 g. This group provided partial permeability while maintaining noticeable restrictions relative to the lasure-coated samples.

High-MW polyol formulations like S4 and S5 displayed permeability approaching those of the lasure layer SMW_{LS}. SMW_{S4S} stabilized at 153.7 h with G = 0.00082 g/h and $\delta = 1.03 \times 10^{-14}$, whereas SMW_{S5S} recorded G = 0.00113 g/h and $\delta = 1.42 \times 10^{-14}$, reaching the steady state at 140.8 h. When analyzed against SMW_{LS}, it is confirmed that S1, S2, and AX, have a barrier behavior similar to SMW_{AJS} for water vapor diffusion. At the same time, S4 and S5 have similar properties; layer-like SMW_{LS}, allowing water vapor to diffuse through the adhesive layer. Polyol S3 had the special well-equilibrated behavior, between partially hindering water diffusion whilst allowing a convenient water vapor diffusion through the adhesive layer. This tiered behavior underscores how the MW of the polyol matrix conveniently controls micro-porosity, and consequently, vapor transmission through the adhesive layer. The relationship between polymer molecular weight and diffusion behavior has also been observed in previous adhesive systems, where increasing molecular weight modified polymer network density and transport resistance [23].

3.2. Water Vapor Diffusion for SMW in the Pre-Steady Zone

For SMW_P, the diffusion process consisted of an initial pre-steady stage lasting till point A_N, at 203.8 h, with a corresponding mass change of 11.36 g. In contrast, the SMW_{AJP} reached the transition point to the steady zone earlier, at A_{AJ} = 115.4 h, with a mass change of 1.05 g. The G and δ values were as shown in Table 2, representing an 84% reduction in permeability capacity relative to SMW. A one-way ANOVA revealed a statistically significant difference in the water vapor permeability coefficient δ between SMW_P and SMW_{AJP} ($F(1, 8) \approx 96$, $p < 0.012$), confirming the pronounced diffusion-hindering effect of the adhesive layer during the pre-steady phase.

This earlier stabilization, despite lower permeability, reflects the restricted diffusion pathways within the adhesive layer. A similar phenomenon has been described in wood–adhesive interfaces where limited capillary pathways led to rapid stabilization of vapor transport despite reduced permeability [8,24]. Due to the limited number of effective capillary channels, vapor diffusion reached its maximum capacity rapidly; beyond this point, no further increase occurred, leading to a quicker transition into steady state.

For SMW_{LS}, the transition point occurred at A_L = 249.6 h, with a mass change of 7.33 g. Compared with SMW, the mass change at point A_L, being its y_A coordinate, was about 1.5 times lower, whereas the mass change at A_{AJ} was less than 15% of A_L. These results confirm that lasure coatings allow partial vapor transmission, reducing but not completely blocking diffusion. Comparable findings were reported for coating systems applied to wood, which typically act as diffusion-retarding rather than diffusion-blocking layers [22,25]. On the other hand, the SMW coated with a different MW adhesive formulation exhibited distinct water vapor diffusion behaviors, particularly in the pre-steady-state zone. As shown in Figure 4 and Table 2, the sample treated with adhesive resin with different MW S1–S5 exhibited variable diffusion patterns depending on the average MW of the resin. In general, S1 (2000 Da), S2 (3000 Da), S3 (4000 Da), S4 (5000 Da), S5 (6000 Da), and AX adhesive type showed reduced vapor diffusion compared with the SMW. The low-MW systems, such as SMW_{S1P}, as shown in Table 2 for diffusion parameters G or δ, demonstrated strong vapor-blocking capacity compared with SMW. The water vapor permeability of SMW_{S1P} and SMW_{AXP} was reduced by approximately 78% and 84%, respectively, relative to SMW_{LP}. Their mass changes at A point were also significantly lower: SMW_{S1P} reached only about 15% of the mass change in SMW_{LP}, while SMW_{AXP} was about 13%.

In comparison with SMW_{AJP}, both SMW_{S1P} and SMW_{AXP} exhibited lower water vapor permeability, as shown in Table 2, with reductions of approximately 27% and 49%, respectively. Intermediate molecular weight formulations demonstrated moderate permeability behavior. For instance, SMW_{S2P} and SMW_{S3P} showed permeability levels corresponding to approximately 40–63% of the SMW_{LP} reference, indicating partial vapor transmission and a semi-permeable diffusion behavior.

Their mass change values at the A point were reduced by 63–74% compared with SMW_{LP}, confirming partial but controlled vapor transmission. By contrast, the higher MW systems, such as SMW_{S4P}, which depended on diffusion parameters as shown in Table 2, and A_{S4} = 153.7 h with mass change = 3.859 g, and SMW_{S5P}, A_{S5} = 140.8 h with mass change = 5.586 g, showed a significant increase in permeability capacity relative to SMW_{LP}. Specifically, SMW_{S5P} exhibited ~35% higher permeability, whereas SMW_{S4P} was about 14% lower than the water vapor permeability of SMW_{LP}. However, both SMW_{S4p} and SMW_{S5p} developed cracking during testing, attributed to strain concentrations along the adhesive layer. Overall, low-MW systems like S1 acted as strong vapor barriers comparable to SMW_{AJP} and SMW_{AXP}, while high-MW systems (S4, S5) allowed excessive permeability. The intermediate formulations (S2, S3), however, proved the most suitable for SMW_{AJ}, offering a balanced molecular weight and a diffusion capacity close to lasure.

Although the steady- and pre-steady diffusion parameters (G and δ) indicate differences between coated and uncoated samples, their slope-based nature limits their ability to fully reflect the actual blocking efficiency of the adhesive layers. Since permeability is calculated as a mass change per unit time, a large mass increase over a long period may numerically resemble a small mass increase over a shorter period, leading to comparable rate values despite fundamentally different diffusion behaviors. This effect is evident when comparing the steady-to-pre-steady ratios of the uncoated SMW and SMW_L, which appear proportionally similar, despite their total accumulated masses differing substantially. For example, at the transition point A, the y_A coordinate of SMWS reached 11.36 g, whereas SMW_{AJS} reached only 1.05 g and SMW_{AXS} 0.95 g, corresponding to an absolute difference of approximately 10.3–10.4 g. Such a large disparity directly reflects the adhesive layer's effective vapor-blocking action. In contrast, when evaluating the late-stage slope between 350 and 400 h (Δm/50 h), the calculated rate values for S1–S5 and AX become relatively close, which does not proportionally represent their markedly different accumulated mass levels. This confirms that slope-derived parameters alone cannot adequately describe the hindering or promoting effect of adhesive systems. Therefore, the y_A coordinate of point A, representing the total mass uptake at the diffusion transition, provides a more physically meaningful and sensitive indicator for assessing adhesive-induced diffusion blocking in SMW.

4. Conclusions

The commercial structural adhesive was identified to act as an effective water vapor barrier. SMW_{AJ} exhibited approximately 7- and 15-fold lower permeability than uncoated SMW in the pre-steady and steady regions, respectively. Similarly, SMW_{AX} showed approximately 12-fold lower permeability than uncoated SMW in both pre-steady and steady regions.

The SMW_{LS} exhibits semi-permeable behavior. SMW_{LS} reached 24.5 times higher than SMW_{AJS}, with AL 249.6 h with a reduced mass change of 7.33 g. and the permeability coefficient exhibited 1.8-fold lower permeability than uncoated SMW in pre-steady zone

The MW of the adhesive is the governing parameter controlling water vapor diffusion; low-MW polyol systems like S1 and S2 exhibited strong diffusion hindrance, comparable to that of the commercial adhesive SMW_{AJS}. Intermediate-MW adhesive formulations like S3 provided partial diffusion capacity, representing a diffusion level between vapor-blocking adhesives and lasure-coated samples. High-MW adhesive systems (S4 and S5) allowed significantly increased vapor diffusion.

It was evidenced that by adjusting the MW of the MDI-based adhesives, it is possible to offer control over the water vapor diffusion of the structural wood adhesives.

The pre-steady diffusion zone revealed markedly stronger contrasts in water vapor diffusion behavior in SMW than the steady-state regime. In this zone, SMW coated with the commercial structural adhesive exhibited an approximately 84% reduction in vapor diffusion compared with uncoated SMW, reaching diffusion saturation at an early stage despite substantially lower mass uptake. In contrast, the steady-state regime showed considerably smaller relative differences for the same SMW configurations, which may obscure the actual vapor-hindering or vapor-supporting performance of the applied surface layers. These findings demonstrate that relying solely on steady-state diffusion parameters, as prescribed by ISO 12572 and ASTM E96, may lead to incomplete conclusions, whereas analysis of the pre-steady zone provides a more sensitive and physically meaningful assessment of early moisture transport mechanisms in SMW and therefore should be considered alongside steady-state evaluation.

Author Contributions: Conceptualization, O.S.Z. and C.C.; formal analysis, O.S.Z. and C.C.; writing—original draft preparation, O.S.Z.; supervision, C.C. All authors have read and agreed to the published version of the manuscript.

Funding: This article was made in frame of the project TKP2021-NKTA-43 which has been implemented with the support provided by the Ministry of Culture and Innovation of Hungary from the National Research, Development and Innovation Fund, financed under the TKP2021-NKTA funding scheme.

Informed Consent Statement: Not applicable.

Data Availability Statement: The original contributions presented in this study are included in the article. Further inquiries can be directed to the corresponding author.

Conflicts of Interest: The authors declare no conflicts of interest.

Abbreviations

A_{AJ}	transition point (A) for Smaragdfa wood samples coated with structural adhesive
A_{AX}	transition point (A) for Smaragdfa wood samples coated with custom-made adhesive
AJ	Structural Adhesives JOWAPUR 681-60
A_L	transition point (A) for Smaragdfa wood samples coated with lasure
A_N	transition point (A) for uncoated Smaragdfa wood samples
A_{S1}	transition point (A) for Smaragdfa wood samples coated with custom-made synthesized resin series 1
A_{S2}	transition point (A) for Smaragdfa wood samples coated with custom-made synthesized resin series 2
A_{S3}	transition point (A) for Smaragdfa wood samples coated with custom-made synthesized resin series 3
A_{S4}	transition point (A) for Smaragdfa wood samples coated with custom-made synthesized resin series 4
A_{S5}	transition point (A) for Smaragdfa wood samples coated with custom-made synthesized resin series 5
ASTM	american society for testing and materials
AX	custom-made adhesive XP 1166
CLT	cross-laminated timber
EWPs	engineered wood products
G	water vapor flow rate
GMO	genetically modified organism
ISO	international organization for standardization
MDI	methylene diphenyl isocyanate
MW	molecular weight
PPG	polypropylene glycol
PUR	polyurethane adhesive
SMA	Smaragdfa wood coated with adhesive
SMW	Smaragdfa wood
SMW_{AJ}	Smaragdfa wood samples coated with structural adhesives
SMW_{AX}	Smaragdfa wood samples coated with custom-made adhesive
SMW_L	Smaragdfa wood samples coated with lasure
SMW_{S1}	Smaragdfa wood samples coated with custom-made synthesized resin series 1
SMW_{S2}	Smaragdfa wood samples coated with custom-made synthesized resin series 2
SMW_{S3}	Smaragdfa wood samples coated with custom-made synthesized resin series 3
SMW_{S4}	Smaragdfa wood samples coated with custom-made synthesized resin series 4
SMW_{S5}	Smaragdfa wood samples coated with custom-made synthesized resin series 5
δ	water vapor permeability

References

1. Clements-Croome, D. Sustainable Intelligent Buildings for People: A Review. *Intell. Build. Int.* **2011**, *3*, 67–86. [CrossRef]
2. Gustavsson, L.; Madlener, R.; Hoen, H.F.; Jungmeier, G.; Karjalainen, T.; Klöhn, S.; Mahapatra, K.; Pohjola, J.; Solberg, B.; Spelter, H. The Role of Wood Material for Greenhouse Gas Mitigation. *Mitig. Adapt. Strateg. Glob. Change* **2006**, *11*, 1097–1127. [CrossRef]

3. Gereke, T. Moisture-Induced Stresses in Cross-Laminated Wood Panels. Ph.D. Thesis, University of Leipzig, Leipzig, Germany, 2009.
4. Lennart, S.; Elina, B. Cellulose Structural Arrangement in Relation to Spectral Changes in Tensile Loading FTIR. *Cellulose* **2009**, *16*, 975–982. [CrossRef]
5. Rafsanjani, A.; Derome, D.; Carmeliet, J. The Role of Geometrical Disorder on Swelling Anisotropy of Cellular Solids. *Mech. Mater.* **2012**, *55*, 49–59. [CrossRef]
6. Ivaniuk, A.; Zayachuk, V.; Lysiuk, R.; Kharachko, T.; Lisoviy, M. Physical and Mechanical Properties of *Paulownia tomentosa* (Thunb.) Steud. Wood under the Conditions of the Western Forest-Steppe of Ukraine. *For. Ideas* **2023**, *29*, 168–180.
7. Barbu, M.C.; Tudor, E.M.; Buresova, K.; Petutschnigg, A. Assessment of Physical and Mechanical Properties Considering the Stem Height and Cross-Section of *Paulownia tomentosa* (Thunb.) Steud. *x elongata* (S.Y.Hu) Wood. *Forests* **2023**, *14*, 589. [CrossRef]
8. Kläusler, O.; Clauß, S.; Lübke, L.; Trachsel, J.; Niemz, P. Influence of Moisture on Stress-Strain Behaviour of Adhesives Used for Structural Bonding of Wood. *Int. J. Adhes. Adhes.* **2013**, *44*, 57–65. [CrossRef]
9. Wadsö, L. Studies of Water Vapor Transport and Sorption in Wood. Ph.D. Thesis, Lund University, Lund, Sweden, 1993.
10. Pfriem, A. *Untersuchungen Zum Materialverhalten Thermisch Modifizierter Hölzer Für Deren Verwendung Im Musikinstrumentenbau*; Institut für Holz- und Papiertechnik der TU: Dresden, Germany, 2007.
11. Pournou, A. Wood Anatomy, Chemistry and Physical Properties. In *Biodeterioration of Wooden Cultural Heritage: Organisms and Decay Mechanisms in Aquatic and Terrestrial Ecosystems*; Springer: Berlin/Heidelberg, Germany, 2020; pp. 1–41.
12. István, K.M.; Csilla, C.; Miklós, B. *Investigation of the Suitability of Smaragdfa for Window Manufacturing*; University of Sopron: Sopron, Hungary, 2023.
13. Temiz, A.; Yildiz, U.C.; Aydin, I.; Eikenes, M.; Alfredsen, G.; Çolakoglu, G. Surface Roughness and Color Characteristics of Wood Treated with Preservatives after Accelerated Weathering Test. *Appl. Surf. Sci.* **2005**, *250*, 35–42. [CrossRef]
14. Slabejova, G.; Fekiac, J.; Panek, M. Influence of Selected Factors on Colour Change of Transparent Finishes on Beech Wood. *Acta Fac. Xylologiae Zvolen* **2014**, *56*, 23–30.
15. *ISO 12572:2016*; Hygrothermal Performance of Building Materials and Products—Determination of Water Vapour Transmission Properties—Cup Method. International Organization for Standardization: Geneva, Switzerland, 2016.
16. *ASTM E96/E96M-16*; Standard Test Methods for Water Vapor Transmission of Materials. ASTM International: West Conshohocken, PA, USA, 2016.
17. Fick, A. Ueber Diffusion. *Ann. Phys.* **1855**, *170*, 59–86. [CrossRef]
18. Robert, H.F. Wood as a Sustainable Building Material. In *Wood Handbook Wood as an Engineering Material Centennial*; Forest Products Laboratory | United States Department of Agriculture Forest Service: Madison, WI, USA, 2010; pp. 1–6.
19. Tetens, O. Uber Einige Meteorologische Begriffe. *Z. Geophys.* **1930**, *6*, 297–309.
20. Sonderegger, W.; Niemz, P. Thermal Conductivity and Water Vapour Transmission Properties of Wood-Based Materials. *Eur. J. Wood Wood Prod.* **2009**, *67*, 313–321. [CrossRef]
21. Wimmer, R.; Kläusler, O.; Niemz, P. Water Sorption Mechanisms of Commercial Wood Adhesive Films. *Wood Sci. Technol.* **2013**, *47*, 763–775. [CrossRef]
22. Viitanen, H.; Ritschkoff, A.-C. Coating and Surface Treatment of Wood. In *Preliminary Material*; Wageningen Academic: Leiden, The Netherlands, 2011; pp. 463–488.
23. Petrie, E.M. *Handbook of Adhesives and Sealants*; McGraw-Hill Handbooks; McGraw-Hill: Columbus, OH, USA, 2000.
24. Hagentoft, C.-E. *Introduction to Building Physics*; Studentlitteratur: Lund, Sweden, 2001.
25. Glass, S.; Zelinka, S. Moisture Relations and Physical Properties of Wood. In *Wood handbook—Wood as an Engineering Material*; General Technical Report FPL-GTR-282; Forest Products Laboratory | United States Department of Agriculture Forest Service: Madison, WI, USA, 2021; pp. 1–4.